Published in final edited form as:
Anal Chem. 2013 December 3; 85(23): 11576–11584. doi:10.1021/ac402777k.

Mass Spectrometry Imaging for Dissecting Steroid Intracrinology within Target Tissues

Diego F. Cobice[a], **C. Logan Mackay**[b], **Richard J. A. Goodwin**[c], **Andrew McBride**[a], **Patrick R. Langridge-Smith**[b], **Scott P. Webster**[a], **Brian R. Walker**[a], and **Ruth Andrew**[a,1]

[a]University/British Heart Foundation Centre for Cardiovascular Science, Queen's Medical Research Institute, University of Edinburgh, 47 Little France Crescent, Edinburgh, EH16 4TJ, UK.

[b]SIRCAMS, School of Chemistry, Joseph Black Building, The King's Buildings, University of Edinburgh, West Mains Road, Edinburgh, EH9 3JJ, U.K.

[c]AstraZeneca R&D, Alderley Park, Macclesfield SK10 4TF, UK.

Abstract

Steroid concentrations within tissues are modulated by intracellular enzymes. Such 'steroid intracrinology' influences hormone-dependent cancers and obesity, and provides targets for pharmacological inhibition. However, no high resolution methods exist to quantify steroids within target tissues. We developed mass spectrometry imaging (MSI), combining matrix assisted laser desorption ionization with on-tissue derivatization with Girard T and Fourier Transform Ion Cyclotron Resonance Mass Spectrometry, to quantify substrate and product (11-dehydrocorticosterone and corticosterone) of the glucocorticoid-amplifying enzyme 11β-HSD1. Regional steroid distribution was imaged at 150-200μm resolution in rat adrenal gland and mouse brain sections, and confirmed with collision induced dissociation/liquid extraction surface analysis. In brains of mice with 11β-HSD1 deficiency or inhibition, MSI quantified changes in sub-regional corticosterone/11-dehydrocorticosterone ratio, distribution of inhibitor, and accumulation of the alternative 11β-HSD1 substrate, 7-ketocholesterol. MSI data correlated well with LC-MS/MS in whole brain homogenates. MSI with derivatization is a powerful new tool to investigate steroid biology within tissues.

Keywords

Mass Spectrometry Imaging; Intracrinology; Glucocorticoids; 11β-HSD1

Introduction

Measurement of steroid hormone concentrations in plasma over more than 50 years has revealed the intricate control of their secretion from endocrine glands. In recent decades, it

[1]Address reprint requests to Dr Ruth Andrew, Address (a) as above Tel: +44 (0) 131 242 6763 Fax: +44(0) 131 242 6779 Ruth.Andrew@ed.ac.uk.

"Supporting Information Available: This material is available free of charge via the Internet at http://pubs.acs.org."

Conflict of interest DFC, CLM, RJAG, AM, PRLS and RA do not have any conflict of interest. BRW and SPW are inventors on patents owned by the University of Edinburgh relating to 11β-HSD1 inhibitors.

Europe PMC Funders Author Manuscripts

has been recognized that steroid concentrations within tissues are also modulated, independently of circulating steroid concentrations, by local steroid-generating and inactivating enzymes. This has been confirmed in spontaneous human enzyme deficiency syndromes, recapitulated by genetic deletion in mice and using pharmacological inhibitors; examples include amplification of estrogen action by aromatase [1], androgen action by 5α-reductase type 2 [2], and glucocorticoid action by 11β-HSDs.[3] Dysregulation of steroidmetabolizing enzyme expression is thought important in the pathophysiology of steroid-dependent disease, including breast cancer, prostate disease and obesity. Moreover, inhibitors of these enzymes have proved useful to reduce steroid action in these disorders. A key limitation in this established field of 'steroid intracrinology', however, is the inability to study steroid concentrations within tissues, particularly in organs with region-specific expression of relevant enzymes, such as the brain, or within heterogeneous samples, such as from cancers. Inferences of the consequences of enzyme (dys)regulation and inhibition for local steroid concentrations therefore remain qualitative rather than quantitative.

Mass spectrometry is widely regarded as the Gold Standard for steroid quantification in plasma. Mass spectrometry imaging (MSI) and Liquid extraction surface analysis (LESA) have recently been developed to map spatial distribution of molecules in tissues allowing localization, detection, identification and quantitation of compounds in complex biological matrices.[4] The distribution of cholesterol, chemically similar to steroids, has been imaged in brain[5,6] and in liver [7] while corticosteroids and androgens have been detected in a non-biological matrix by cation-enhanced nanostructure-initiator mass spectrometry.[8] However, localization of endogenous neutral steroids in biological tissues by MSI is challenging, not only because of their relatively low abundance, but also because of their lack of either hydrogen donor or acceptor moieties, resulting in poor ionization yields during matrix assisted laser desorption (MALDI). Furthermore, steroids are susceptible to ion suppression by more abundant molecules, such as lipids and proteins. Although steroids can be ionized by conventional electrospray or APCI [9], detection in the low sub-pg range in tissues is largely out of reach, and these quantitative approaches do not offer two-dimensional imaging. For electrospray ionization (ESI), derivatization [10,11] enhances the ionization efficiency of neutral corticosteroids, for example using Girard reagents. [12] Similar approaches have allowed Girard P (GirP) derivatives of oxysterols to be detected with fmole sensitivity in rat brain homogenates using MALDI [13], and have enhanced sensitivity for cholesterol analysis using N-alkylpyridinium isotope quaternization in analysis of human hair homogenate by MALDIFTICR. [14] The recent innovation of on-tissue chemical derivatization (OTCD) [15,16] has paved the way for application of derivatization techniques to MSI for investigation of tissue steroids.

We aimed to develop MSI initially for analyzing corticosteroids. The major glucocorticoid in rodents, corticosterone (CORT), is relatively abundant and, in addition to its secretion from the zona fasciculata of the adrenal cortex, is also generated within target tissues from the inert precursor 11-dehydrocorticosterone (11DHC) by the enzyme 11β-HSD1. [3] Inhibition of 11β-HSD1 in brain is associated with improved memory [17,18] but the consequences for local steroid concentrations in the brain sub-regions where 11β-HSD1 is expressed are uncertain. Moreover 11β-HSD1 can interconvert other keto and hydroxy substrates [19-22], including 7-keto and 7β-hydroxycholesterol, but it has been difficult to

establish the equilibrium of these reactions *in vivo*. We have applied OTCD, in combination with MSI, for the first time to quantify and validate the detection of CORT and 11DHC and alternative substrates within sub-regions of murine brain. Neutral steroids were converted to positively charged hydrazones derivatives using Girard reagents T (GirT), enabling detection and quantitation by MALDI and LESA with Fourier transform Ion cyclotron MSI (MALDI-FTICR-MSI). Validation was performed with LC-MS/MS. MSI demonstrated alterations in brain glucocorticoids (and 7-ketocholesterol, an alternative substrate) in mice with 11β-HSD1 deficiency, and allowed simultaneous pharmacokinetic/pharmacodynamic studies with an 11β-HSD1 inhibitor. A potent, selective and orally bioavailable piperidinyl-pyrazol inhibitor of 11β-HSD1 (UE 2316) was used; UE 2316 crosses the blood-brain barrier and displays potency across species (IC50, (mouse, 162 nM), (rat 80nM).[23]

Materials and Methods

Chemicals and reagents

Internal standard (ISTD) corticosterone-2,2,4,6,6,7α,21 (d_8CORT) (purity 95-97%) (Cambridge Isotopes; MA, USA); 11-dehydrocorticosterone (11DHC) (Steraloids Inc, PA, USA); UE2316, [4-(2-chlorophenyl-4-fluoro-1-piperidinyl][5-(1H-pyrazol-4-yl)-3-thienyl]-methanone and UE2346 were synthesized by High Force Ltd, UK.[23] Solvents were glass-distilled HPLC grade (Fisher Scientific, Loughborough, UK). 4-Chloro-α-cyanocinnamic acid (Cl-CCA) was synthesized in-house.[24] All other chemicals were purchased from Sigma-Aldrich (Dorset, UK) unless otherwise stated.

Animals and biomatrix collection

Licensed procedures were performed under the UK Animals (Scientific Procedures) Act, 1986. Sprague Dawley male rats (5-7 weeks, ~175-200g, source of adrenal glands) and C57BL/6 mice (6-7 weeks, male) were from Harlan Olac Ltd (Bicester, UK). 11β-HSD1$^{-/-}$ mice (KO) and their wild-type (WT) littermates (male, 2-3 months) were bred in-house. [24] The genetically modified animals were obtained from in house breeding colony and were slightly older than commercial stock; however, age-matched controls were used in each experiment. In all studies, animals were killed by decapitation at 09:00 h, plasma was prepared from trunk blood, collected in EDTA. Tissues were snap frozen in liquid nitrogen and stored (−80°C).

Tissue sectioning and mounting

The cryostat (Leica Microsystems Inc, Bannockburn, IL, USA) was cleaned and tissue embedded in gelatine solution 10%*w/v*. Coronal/horizontal brain and adrenal cryosections (10 μm) were cut and frozen (−80°C), adapted from Koeniger.[25] Briefly: (1) fifteen tissue sections (50 μm thick) were collected for confirmatory quantitation; (2) two adjacent sections were thaw mounted onto glass slides (Superfrost, Thermo Scientific, Braunschweig, Germany) and retained for histological examination; (3) four adjacent sections for MSI/LESA (10 μm) were thaw mounted onto a conductive indium tin-oxide (ITO)-coated glass slides (Bruker Daltonics, Bremen, GmbH) pre-coated with GirT-reagent (0.15mg/cm^2) and further sections for histology (x2) and confirmatory quantitation (x15) were harvested as above. Tissue sections for confirmatory quantitation were combined, weighed at room

temperature (RT) and stored at −80°C until LC-MS/MS analysis. Tissue sections for MSI were stored in a vacuum desiccator (RT, 1h) and then at −80°C.

Instrumentation

MSI was performed using a 12T SolariX MALDI-FTICR-MS (Bruker Daltonics, MA, US) employing a Smartbeam 1 kHz laser, with instrument control using SolariX control v1.5.0 (build 42.8), Hystar 3.4 (build 8) and FlexImaging version 3.0 (build 42). On-tissue collision induced dissociation was carried out by Liquid extraction surface analysis (LESA)-nanoESI-FTICR-MS using Triversa nanomate® (Advion, NY, USA). Confirmatory liquid chromatography-tandem MS (LC-MS/MS) analysis was performed using a triple-quadrupole linear ion trap mass spectrometer (QTRAP 5500, AB Sciex, Cheshire, UK) coupled with an ACQUITY ultra high pressure liquid chromatography (UPLC; Waters, Manchester, UK).

MALDI-FTICR-MSI analysis

Optical images were taken using a flatbed scanner (Cannon LiDE-20, Cannon, UK). MSI analysis was performed using 250 laser shots, with a laser spot diameter of ~50 μm and laser power was optimized for consistent ion production. Ions were detected between *m/z* 250 and 1500, yielding a 1 Mword time-domain transient, and with a laser spot raster spacing of 100 – 300 μm unless otherwise stated. MSI data were subject to vector normalization method (RMS) at 0.995 as ICR noise reduction threshold. Mass precision was typically ± 0.025 Da. Average abundances were determined by defining specific regions of interest (ROI). A measure of the average abundance was then assigned from the summed spectra. Neutral steroids were analyzed (without application of derivatization reagent) in positive and negative ion modes at +ve *m/z* 345.20604, −ve *m/z* 343.19148 for 11DHC and +ve *m/z* 347.22169, −ve *m/z* 345.20604 for CORT. Ions formed by the derivatives were monitored in positive mode, with +ve *m/z* 458.30133 (GirT-11DHC) and +ve *m/z* 460.31698 (GirT-CORT) and +ve *m/z* 468.36718 (GirT-d_8CORT). UE2316 was monitored at +ve *m/z* 390.08377 and GirT-7 ketocholesterol (GirT-7KC) was monitored at +ve *m/z* 514.43670. α-Cyano-4-hydroxycinnamic acid (CHCA) matrix ion at +ve *m/z* 417.04834 was also monitored to assess matrix application uniformity and perform an internal calibration.

On-tissue chemical derivatization (OTCD)

From −80°C, tissues were allowed to dry in a vacuum desiccator (20 mins). The GirT pre-coated glass slide (0.15mg/cm^2) was sprayed with 2ml of methanol containing 0.2% v/v of TFA, then it was placed in a sealed Petri dish (or similar container) containing moist tissue paper to create a moisturizing reaction environment. Two ml of distilled water was enough to produce a suitable reaction media; more water may cause analyte delocalization due to derivatisation reagent diffusion. The moist kim-wipe tissue was placed around the inner walls of the container without touching the glass slide. The tissue was the incubated (60min, 40°C) in an oven or water bath, then allowed to cool and dry in a vacuum desiccator (RT, 15min) to remove the condensed water prior to matrix deposition as above. Other derivatisation reagents were evaluated such as isonicotinoyl and sulfonyl chlorides among

other hydrazine reagents. Details of optimization and derivatisation screening are in Supplementary Information, Table S1.

Matrix application

Matrix (CHCA; 10mg/mL) in acetonitrile (80%)) + 0.2% v/v TFA) was applied by a pneumatic TLC sprayer (20mL per slide with a nitrogen flow of 7.5L/min at a distance of 20 cm from the MALDI target). Each manual pass took approximately 1 second and the process was repeated with 5-10s between passes until a uniform matrix coating was achieved on the tissue section. The tissue section was then allowed to dry (RT) and stored in a desiccator until analysis.

Detection of endogenous steroids in murine tissue using derivatization

Steroids were imaged in adrenal glands from Sprague Dawley rats and brains from C57Bl/6 mice (n=6/tissue). Tissues were prepared, derivatized as described and matrix applied. Steroid derivatives were imaged by MALDI-FTICR-MS.

Histological staining

Cryosections were stained using haematoxylin and eosin.[26] After fixation in cold acetone, tissue sections were examined using an optical microscope (40X, Leica Microsystems Inc, Bannockburn, IL, USA) with CCD camera (Hitachi model 3969, Japan).

Liquid extraction surface analysis (LESA)-ESI-FTICR-MS

This was performed in both adrenal and brain sections. Steroids within tissue sections were derivatized as previously described and analyzed immediately using LESA-nanoESI-FTICR-MS as follows: solvent (methanol: water, 50:50 with 0.1% v/v of formic acid), pick-up volume: 1.5 μL, dispense volume, 1.2 μL at 0.2mm away for surface, droplet rest time (delay) 5 seconds and aspiration volume of 1.4μL at 0.0mm away from surface. ESI-FTICR-MS was performed using the 12T SolariX dual source (ESI-MALDI) with SolariX control v1.5.0 (build 42.8). Ions were detected between *m*/*z* 250-1500, yielding a 2 Mword time-domain transient. Ions of GirT-hydrazones (as for MALDI analysis above) were isolated for 30 sec prior to isolation (*m*/*z* 460.3±5Da) and CID experiments. CID was carried out using 28 eV as collision energy.

Confirmatory analysis by LC-MS/MS

Analysis of corticosteroids (adapted from Wang) [13] and UE2316 in murine brain were performed using LC-MS/MS in multiple reaction monitoring mode (MRM), for method details see supporting information.

Influence of 11β-HSD1 on amounts of active and inactive glucocorticoids in brain tissue

The effect of deficiency of the 11β-HSD1 enzyme was studied using 11β-HSD1$^{-/-}$ (knockout, KO) mice and their wild-type littermates (n=6/group) and after pharmacological inhibition of 11β-HSD1 in C57BL/6 mice (n=6/group, killed 1h, 4hs and 6hs after receiving UE2316 (20mg/kg oral, in DMSO: PEG-400: saline (0.9%*w*/*v*) (2:38:60)) or vehicle).

Tissues were harvested at cull and MSI performed as described. The identities of ions of the steroid-GirT hydrazones were confirmed on-tissue by CID using LESA. The average spectral intensities of steroid derivatives in ROIs across the cortex, hippocampus and amygdala were recorded using MSI, presented as ratios of CORT/11DHC and compared with those generated by LESA and LC-MS/MS.

Statistical analysis

Data are expressed as mean ± SEM and differences were analyzed using two-way ANOVA with Fisher's post-hoc test (MSI and LESA) and Student's t-test (LC-MS/MS). Statistical significance was accepted at $p < 0.05$. Statistical calculations were performed using Statistica® version 8.0, StatSoft, Inc.Tulsa, OK, USA. Data generated by different analytical methods were compared by Bland-Altman plots.

Structure drawing

Molecular structure drawing was performed using MarvinSketch 5.4.0.1, Chemaxon Ltd, Budapest, Hungary.

Results

OTCD-MALDI-FTICR-MSI method development and optimization

To detect corticosterone (CORT) and 11-dehydrocorticosterone (11DHC), standards were analyzed by MALDI mass spectrometry. $[M+H]^+$ pseudomolecular ions were the most abundant ions detected when standards of corticosterone (CORT) and 11-dehydrocorticosterone (11DHC) were analyzed, with masses at *m*/*z* 347.22101 and *m*/*z* 345.20632, in close agreement with the theoretical masses *m*/*z* 347.22169 and *m*/*z* 345.20604 respectively (Figure S1a,b); ions due to dehydration were not observed. Initial imaging attempts in adrenal tissue, monitoring only the $[M+H]^+$ ion of the glucocorticoids of interest, yielded ions with mass accuracy of −3.2 ppm (CORT) and −18.3ppm (11DHC) (Figure S1c,e,f,h,i) but with low signal to noise ratio. Limits of detection (LODs) of CORT and 11DHC were ~ 30ng (off-tissue) and 1μg (on-tissue).

To improve images of neutral steroids in tissues, a number of approaches were pursued to enhance their low intensity signal. Initially matrix screening was performed using both standard and novel matrices, to identify reagents which may enhance energy transfer. Substantial differences were observed between matrices; the maximum signal intensity and desorption yield was achieved using CHCA (Figure S2a). Interestingly, the novel 4-chloro-α-cyanocinnamic acid (Cl-CCA), which possesses a lower proton affinity than its hydroxyl analogue and increased the signal of poorly ionizable peptides [27], demonstrated lower intensity signals in combination with steroids than CHCA, although the background signal was noticeably lower in the low mass range (200-400 Da). Despite using CHCA, the LOD did not reach the required sub-pg levels of endogenous corticosteroids in tissue.

Derivatization was explored by introducing readily ionizable or permanently charged groups, an approach effective in enhancing signal intensity with LC-MS/MS. [11-13] Poor desorption or ionization by MALDI analysis was found using derivatives targeting the

primary (C21) alcohol moiety with acyl and sulfonyl chlorides. Screening derivatization reactions, targeting the α-β unsaturated ketone at C3 in the steroid A-ring (Table S1) improved signal intensity in positive mode when the corticosteroids were converted to derivatives either permanently charged or easily protonated. In particular, formation of a quaternary ammonium derivative, by a hydrazine-type condensation reaction of the ketone at both C3 and C20 to form the water soluble hydrazones group, greatly enhanced response (Table S1).

The highest sensitivity was achieved with derivatives formed using GirT reagent. Derivatives of CORT and 11DHC generated ions of similar intensities, with LODs of 0.01-0.03pg (off-tissue) and 1-0.1pg (on-tissue), and signals of the endogenous CORT and 11DHC in tissues were considerably enhanced (Figure 1c,d). GirT condensation is generally carried out using protic solvents in a weak acid media at room temperature with reaction times around 10-18 hours achieving 60-80% of conversion to hydrazones. [28] Recent studies have shown that the reaction can be carried out in 30min at 70°C. [29,30] However, such as high temperature may cause disruption of tissue morphology due to an increase of water vapor in the reaction chamber and can also lead to diffusion of the water soluble GirT derivatives and ion suppression effects due to protein cleavage and tissue component degradation. The best yield, on-tissue, was achieved in 1h at 40 °C, in a moisturizing environment using methanol/TFA as solvent/catalyst system (Figure S2b). The trifluoroacetate ion may facilitate the derivatisation reagent incorporation due its tissue-penetration properties. Greatest signal intensity was achieved using 4ml of 5mg/ml solution for post-coating and 0.15mg/cm^2 for pre-coating. In the ultimate protocol, slides were pre-coated with defined amounts of reagents, offering the additional benefit of limiting analyte diffusion. The reaction was quenched by dehydration to avoid subsequent hydrolysis. When GirT is used in MS analysis coupled with chromatography, the excess of derivatization reagent is diverted to waste to avoid ion-suppression in the MS ion source. [29] In OTCD this is not practical, so the amount of derivatization reagent was limited to ensure maximum conversion and minimum ion-suppression.

Matrix was deposited using as a spray, and analyte diffusion as well as surface topology and crystal homogeneity were controlled by standardization of all possible variables, such as nitrogen flow, distance from the MALDI target, time between passes and solvent volume. Crystal homogeneity was inspected using light microscopy showing an uniform cocrystallization pattern. An image of the matrix ion was also recorded with each tissue to ensure even application. ”Solvent-free” approaches to apply matrix, such as sublimation and sublimation/recrystallization were evaluated but, in combination with GirT steroids, demonstrated poor signal to noise ratios. As previously reported [31], proteolysis and tissue degradation during sample preparation may cause ion-suppression. With the optimized protocol in place, stability was evaluated temporally by assessing the intensity of signal from GirT-CORT applied on and off tissue sections; only 13% reduction in signal suppression/degradation was observed after 20 minutes at RT, within the necessary limit of tissue handling times (Figure S2c).

GirT derivatives yielded spectra dominated by the molecular ion (Figure S3) and high resolution MS was used to overcome the challenge of selecting specific analytes of interest

from the many high abundance isobaric ions in the low mass range. Structural confirmation by fragmentation using LESA-ESI-FTICR-MS followed by CID, allowed isolation of the precursor ions in the ICR cell, increasing both sensitivity and selectivity. This process provided fragmentation patterns typical of GirT hydrazones (Figure S4), concordant with the structures of steroid hydrazones, extrapolating from GirP analogues, which may form a stable five member ring as previously reported. [13] CID of the GirT derivatives generated a series of fragment ions characteristic of the loss of the quaternary amine tag $[M-59]^+$ and carbon monoxide $[M-87]^+$ of the derivatized group at *m/z* 399, *m/z* 371 (GirT-11DHC) and *m/z* 401, *m/z* 373 (GirT-CORT), respectively. Also, a GirT-CORT selective fragment was observed at *m/z* 383 corresponding to the neutral loss of water at C11 of the *m/z* 401 GirT-CORT fragment ion.

In rat adrenal gland, molecular distribution maps showed GirT-CORT (*m/z* 460.31713) and GirT-11DHC (*m/z* 458.30139) in high abundance in the zona fasciculata/reticularis (Figure 1c, d), with mass accuracy of ±5 ppm from their theoretical monoisotopic masses (Figure 1e-g) and signal to noise ratios >100.

Studies of manipulation of 11β-HSD1

Endogenous CORT (Figure 2b, 2d) and 11DHC (Figure 2c, 2e) were successfully detected as GirT hydrazones by MSI in sections of murine brain from both wild-type (WT) and 11β-HSD1$^{-/-}$ mice. Corticosteroid derivatives were detected in highest abundance in the cortex, hippocampus and amygdala. In 11β-HSD1$^{-/-}$ mice, the CORT/11DHC ratio was reduced in these regions of interest (Figure 2f). Absolute ratios (and magnitude of difference between 11β-HSD1$^{-/-}$ and WT mice) obtained by LCMS/MS and LESA were similar to those determined by MSI (Figure 2f). Absolute measurements (Figure 2g) suggested the change in pattern between genotypes was driven by increased amounts of 11DHC and reduced amounts of CORT, although only the former was statistically significant.

Following a single oral dose of UE2316, an inhibitor of murine 11β-HSD1, levels of the drug detected by MSI peaked in brain one hour post-dose (Figure 3b, vehicle, Figure 3c-e, UE2316); the MSI data were confirmed by LC-MS/MS of drug in whole brain (Figure 3f). The regional distribution of glucocorticoids was similar in brains of vehicle and UE2316 treated mice (Figure 3h,j (CORT), 3i,k (11DHC)) with UE2316 reduced CORT/11DHC ratios measured by MSI in the cortex, hippocampus and amygdala (Figure 3l). Quantitative analysis by LC-MS/MS confirmed these findings (Figure 3m).

Correlation between methods of quantitation

Good agreement was observed between MSI and LC-MS/MS (Figure S5a) and between MSI and LESA (Figure S5b), across the range of values, although MSI-LESA demonstrated a negative bias using Bland-Altman analysis.

Quantitation of alternative substrates of 11β-HSD1

The GirT derivative of 7-ketocholesterol was detected by MSI in brain sections (Figure 4) and its abundance increased in mice with disruption (Figure 4b-d) or inhibition (Figure 4e-g) of 11β-HSD1.

Discussion

This novel application of OTCD coupled with MSI permits detection of poorly ionizable endogenous corticosteroid hormones within tissues, by generating permanently charged derivatives which yield intense signals upon MALDI-FTICR analysis. The spatial distribution of the substrate and product of 11β-HSD1, 11DHC and CORT, in rat adrenal glands and murine brain was visualized. Quantitation in 11β-HSD1 deficient mice allowed assessment of the consequences of regional activity of 11β-HSD1 for local steroid levels, and the approach also allowed pharmacodynamic and pharmacokinetic assessment of an 11β-HSD1 inhibitor within the brain. This technique has the potential to be applied to other steroids and sterols to investigate steroid intracrinology in multiple organs and in solid tumors.

The novel use of GirT reagent permitted low LODs. Similar derivatives have been used to enhance analysis of sterols and steroids by LC-MS/MS (ESI) [10-14,29,30] but there has been limited application of derivatization for tissue imaging, with only two previous examples for non-steroidal small molecules. [15,16] The reaction reported here favored the α-β unsaturated-keto moiety at C3 as the π electrons are delocalized across the conjugated system leaving the carbonyl susceptible to a nucleophilic attack. Indeed monitoring the reaction products for up to 3h did not reveal formation of multiple charged derivatives, indicative of reactions taking place at other positions. The efficiency of OTCD reaction was clearly demonstrated, as the signal intensity was considerable enhanced after conversion of native corticosteroids to their corresponding GirT hydrazones. The transformation of neutral steroid to their corresponding water-soluble and charged derivatives was achieved in a short period of time using a simple customize reaction chamber. The moisturizing environment was controlled by the amount of water and reaction temperature allowing little analyte diffusion. The derivatization allowed mapping the low levels endogenous steroids on both adrenal gland and brain tissue sections. The concept of charge-tagging may be extrapolated to other neutral keto-steroids for the generation of molecular profiles in target tissues, and indeed here was also used successfully to image 7-ketocholesterol.

Rat adrenal glands were selected as a model tissue for method development, and subsequently as a positive control, due to the anticipated high abundance of corticosteroids. Glucocorticoids were visualized and most abundant in the zona fasciculata, the major source of glucocorticoid synthesis, with lower signal in the outer zona glomerulosa, where corticosterone is further metabolized to aldosterone. This confirmed that unwanted diffusion of analytes was constrained by the tissue processing method. Spatial resolution of the laser is adjustable, but increasing the spatial resolution decreases sensitivity as the spot size sampled is smaller. In the adrenal, collecting data at 200μm resolution generated sufficient spatial information with adequate signal (signal/noise >100, compared with signal/noise ~20 at 50μm spatial resolution). In future use of the technique, the spatial resolution may be increased according to the region and tissue of interest, but must be balanced against robustness of signal. Implementation of continuous accumulation of selected ions “CASI™” may facilitate these advances.

OTCD coupled with MALDI-FTICR-MSI was successfully applied in murine brain, where discriminating abundance of glucocorticoids in sub-regions was possible. The highest abundance in cortex, hippocampus and amygdala may reflect the higher expression of corticosteroid-binding receptors as well as of 11β-HSD1 in these brain regions. [32] To evaluate use of the technique to interpret biological variations in tissue steroid levels, proof-of-principle experiments were performed using brains of mice with 11β-HSD1 deficiency or receiving pharmacological 11β-HSD1 inhibitors. Changes in enzyme activity were quantified by CORT/11DHC ratios, which is appropriate since derivatives of both steroids possess similar ionization yields and signal intensities when compared using post-processing vector normalization (RMS). An alternative approach would have been to incorporate a labeled steroid (e.g. d_8CORT) in the matrix, allowing signal intensity to be normalized; this approach also offers the advantage of a further read-out of uniformity of matrix application but was not employed here. Disrupting or inhibiting 11β-HSD1 was anticipated to increase the CORT/11DHC ratio, as previously reported in homogenates of brain from 11β-HSD1 deficient mice. [33] This was detected, and quantified in brain sub-regions, with an increase of the signal intensity of GirT-11DHC and a smaller decline in GirT-CORT levels across the cortex, hippocampus and amygdala with 11β-HSD1 deficiency or inhibition. These brain regions have high abundance of 11β-HSD1 mRNA.[32]

CORT in the brain is derived both from the circulation and from local 11β-HSD1 activity. The proportionate contribution of each source, however, is unknown. To date, this has been inferred for some tissues, imprecisely, from studies using arteriovenous sampling in combination with stable isotope tracers [34], by sampling interstitial fluid by microdialysis [35], or by quantifying steroid concentrations in whole tissue homogenates ex *vivo.* [36] The MSI data here provides the novel insight that there is a small decline of only 16% in active CORT with 11β-HSD1 deficiency in regions of the brain where 11β-HSD1 is normally most highly expressed; suggesting the contribution of 11β-HSD1 to the intracellular pool of corticosterone in these experimental conditions is relatively modest.

Lastly using MSI, it was possible to image alternative substrates of 11β-HSD1, in this case 7-ketocholesterol. Previously it has been difficult to establish whether 11β-HSD1 predominantly reduces 7-ketocholesterol to 7β-hydroxycholesterol or if oxidation dominates. [22] Indeed, changes in the balance of circulating oxysterols are modest in 11β-HSD1$^{-/-}$ mice. By demonstrating accumulation of 7-ketocholesterol with 11β-HSD1 deficiency, MSI has provided clear novel evidence that reduction of oxysterols by 11β-HSD1 predominates.

Conclusions

MSI with on-tissue derivatization is a powerful new tool to study the regional variation in abundance of steroids within tissues. This is the first technique capable of detecting and quantifying corticosteroids to <200μm resolution, and at physiological concentrations, allowing application within region-specific areas of murine brain. We have demonstrated its utility for measuring pharmacodynamic effects of small molecule inhibitors of 11β-HSD1; in combination with pharmacokinetic imaging, this will facilitate screening of the disposition of such drugs being developed to treat Alzheimer's disease. Importantly, this

technique opens the door for expanding the range of steroids that can be studied by MALDI-MSI by adapting existing chemical derivatization methods. In the first instance this may encompass other α-β unsaturated keto steroids, such as testosterone and progesterone, as well as keto-sterols, and may be applied in other tissues such as prostate gland and breast tissue. This offers the prospect of many novel insights into tissue-specific steroid and sterol biology.

Supplementary Material

Refer to Web version on PubMed Central for supplementary material.

Acknowledgements

We are grateful to the British Heart Foundation (DFC, RA, BRW) and the Wellcome Trust (AMcB, BRW, SPW) for funding this work. We thank SIRCAMS and the Mass Spectrometry Core of the Wellcome Trust Clinical Research Facility for technical support. We are also thanking Dr. Gregorio Naredo Gonzalez (Mass Spectrometry Core) for his help in the synthetic chemistry.

References

(1). Simpson ER, Mahendroo MS, Means GD, Kilgore MW, Hinshelwood MM, Graham-Lorence S, Amareh B, Ito Y, Fisher CR, Michael MD, Mendelson CR, Bulun SE. Endocr. Rev. 1994; 15:342–355. [PubMed: 8076586]

(2). Russell DW, Wilson JD. Annual Reviews of Biochemistry. 1994; 63:25–61.

(3). Seckl JR, Walker BR. TEM. 2004; 15:418–424. [PubMed: 15519888]

(4). Heeren RM, Chughtai K. Chem Rev. 2010; 110:3237–3277. [PubMed: 20423155]

(5). Malmberg H, Nygren P, Sjövall L. a. J. L. Spectroscopy. 2013; 18:503–511.

(6). Dufresne M, Thomas A, Breault-Turcot J, Masson J-F, Chaurand P. Anal. Chem. 2013; 85:3318–3324. [PubMed: 23425078]

(7). Winograd N, Garrison BJ. Annu. Rev. Phys. Chem. 2010; 61:305–322. [PubMed: 20055679]

(8). Patti GJ, Woo HK, Yanes O, Shriver L, Thomas D, Uritboonthai W, Apon JV, Steenwyk R, Manchester M, Siuzdak G. Anal. Chem. 2010; 82:121–128. [PubMed: 19961200]

(9). Singh G, Gutierrez A, Xu K, Blair IA. Anal Chem. 2000; 72:3007–3013. [PubMed: 10939360]

(10). Quirke JM, Van Berkel GJ. J. Mass Spectrom. 2001; 36:1294–1300. [PubMed: 11754121]

(11). Higashi T, Yamauchi A, Shimada K. J. Chromatogr. B Analyt. Technol. Biomed. Life Sci. 2005; 825:214–222.

(12). Shackleton C. J. Steroid Biochem. Mol. Biol. 2010; 121:481–490. [PubMed: 20188832]

(13). Wang Y, Hornshaw M, Alvelius G, Bodin K, Liu S, Sjovall J, Griffiths WJ. Anal. Chem. 2010; 78:164–173. [PubMed: 16383324]

(14). Wang H, Wang H, Zhang L, Zhang J, Guo Y. Anal. Chim. Acta. 2011; 690:1–9. [PubMed: 21414431]

(15). Chacon A, Zagol-Ikapitte I, Amarnath V, Reyzer ML, Oates JA, Caprioli RM, Boutaud O. J. Mass Spectrom. 2011; 46:840–846. [PubMed: 21834023]

(16). Manier ML, Reyzer ML, Goh A, Dartois V, Via LE, Barry CE III, Caprioli RM. J. Am. Soc. Mass Spectrom. 2011; 22:1409–1419. [PubMed: 21953196]

(17). de Kloet ER, Joels M, Holsboer F. Nat. Rev. Neurosci. 2005; 6:463–475. [PubMed: 15891777]

(18). Yau JL, Noble J, Seckl JR. J. Neurosci. 2011; 31:4188–4193. [PubMed: 21411659]

(19). Kotelevtsev YV, Brown RW, Fleming S, Edwards CRW, Seckl JR, Mullins JJ. J. Clin. Invest. 1999; 103:683–689. [PubMed: 10074485]

(20). Wamil M, Andrew R, Chapman KE, Street J, Morton NM, Seckl JR. Endocrinology. 2008; 149:5909–5918. [PubMed: 18755798]

(21). Hult M, Elleby B, Shafqat N, Svensson S, Rane A, Jornvall H, Abrahamsen L, Oppermann U. Cell and Molecular Life Sciences. 2004; 61:992–999.

(22). Mitic T, Shave S, Semjonous N, McNae I, Cobice DF, Lavery GG, Webster SP, Hadoke PW, Walker BR, Andrew R. Biochem. Pharmacol. 2013; 86:146–153. [PubMed: 23415904]

(23). Webster SP, Seckl JR, Walker BR, Ward P, Pallin TD, Dyke HJ, Perrior TR. PCT Intl. 2011 WO2011/033255.

(24). Kotelevtsev YV, Holmes MC, Burchell A, Houston PM, Scholl D, Jamieson PM, Best R, Brown RW, Edwards CRW, Seckl JR, Mullins JJ. Proc. Natnl. Acad. Sci. USA. 1997; 94:14924–14929.

(25). Koeniger SL, Talaty N, Luo Y, Ready D, Voorbach M, Seifert T, Cepa S, Fagerland JA, Bouska J, Buck W, Johnson RW, Spanton S. Rapid Commun. Mass Spectrom. 2011; 25:503–510. [PubMed: 21259359]

(26). Heap BJ, Kiernan JA. J. Anat. 1973; 115:315–325. [PubMed: 4762130]

(27). Jaskolla TW, Lehmann WD, Karas M. Proc. Natl. Acad. Sci. U. S. A. 2008; 105:12200–12205. [PubMed: 18723668]

(28). Wheeler O. Chem Rev. 1962; 62:205–221.

(29). Khan AK, Wang Y, Heidelberger S, Avelius G, Liu S, Sjövall J, Griffiths W,J. Steroids. 2006; 71:42–53. [PubMed: 16199070]

(30). Griffiths W,J, Liu S, Avelius G, Sjövall J. Rapid Commun. Mass Spectrom. 2003; 17:924–935. [PubMed: 12717765]

(31). Goodwin RJ, Iverson SL, Andren PE. Rapid Commun. Mass Spectrom. 2012; 26:494–498. [PubMed: 22302488]

(32). Moisan M-P, Seckl JR, Monder C, Agarwal AK, White PC, Edwards CRW. Neuroendocrinology. 1990; 2:853–858.

(33). Sooy K, Webster SP, Noble J, Binnie M, Walker BR, Seckl JR, Yau JLW. The Journal of Neuroscience. 2010; 30:13867–13872. [PubMed: 20943927]

(34). Hughes KA, Manolopoulos KN, Iqbal J, Cruden NL, Stimson RH, Reynolds RM, Newby DE, Andrew R, Karpe F, Walker BR. Diabetes. 2012; 61:1357–1364. [PubMed: 22511204]

(35). Wake DJ, Homer NZM, Andrew R, Walker BR. Journal of Clinical Endocrinology & Metabolism. 2006; 91:4682–4688. [PubMed: 16954164]

(36). Hughes KA, Reynolds RM, Critchley HO, Andrew R, Walker BR. Journal of Clinical Endocrinology & Metabolism. 2013; 95:4696–4702. [PubMed: 20631029]

Europe PMC Funders Author Manuscripts

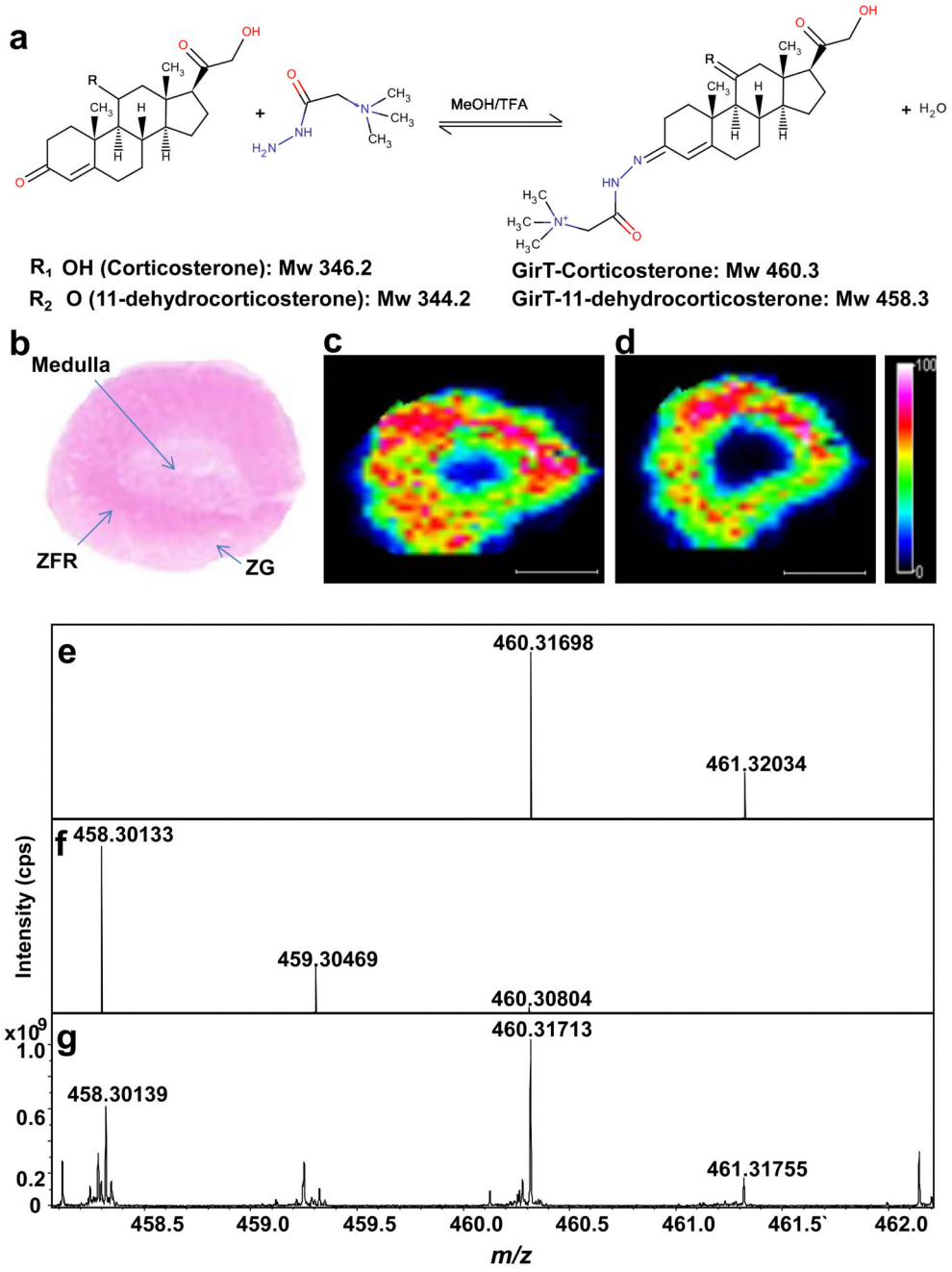

Figure 1. Molecular imaging by MALDI-FTICR-MSI of corticosteroid derivatives prepared with Girard T reagent (GirT) in representative rat adrenal gland sections

Molecular regional distribution maps showed GirT-CORT (*m/z* 460.31713) and GirT-11DHC (*m/z* 458.30139) in high abundance in the zona fasciculata/reticularis (site of glucocorticoids synthesis) with mass accuracy of ±5 ppm from their theoretical monoisotopic masses and (S/N) signal to noise ratios above 100. (**a**) Derivatization of corticosterone and 11-dehydrocorticosterone with GirT. (**b**) Histological image of a cryosection of rat adrenal gland stained with haematoxylin and eosin (ZG = zona glomerulosa; ZFR = zona fasciculata reticularis). Heat map of GirT derivatives of: (**c**)

corticosterone (GirT-CORT) at *m/z* 460.31698±0.025Da; and (**d**) 11-dehydrocorticosterone (GirT-11DHC) at *m/z* 458.30133±0.025Da, collated by MALDIFTICR-MS. Signal intensity is depicted by color on the scale shown. Simulated theoretical isotopic distribution pattern of: (**e**) GirT-CORT; and (**f**) GirT-11DHC. (**g**) Representative FTICR-MS spectrum of corticosteroid hydrazones in rat adrenal gland, showing excellent agreement with theoretical mass. **TFA=** Trifluoroacetic acid. **MeOH** = Methanol. **Mw** = molecular weight (Da). **cps** = counts per second. Scale bar (2mm).

Europe PMC Funders Author Manuscripts

Europe PMC Funders Author Manuscripts

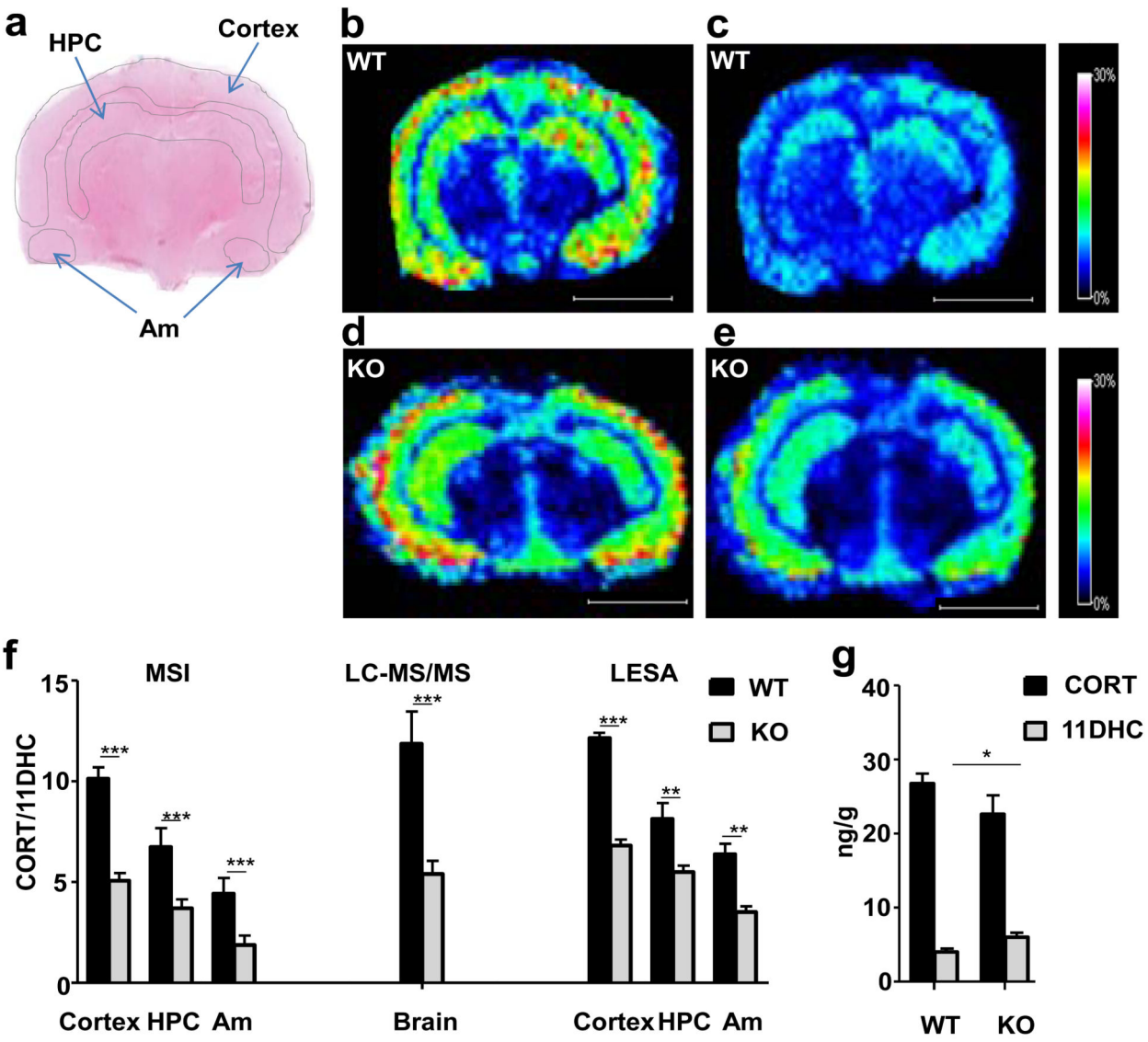

Figure 2. Effect of 11β-hydroxysteroid dehydrogenase type 1 (11β-HSD1) deficiency on proportions of active and inactive glucocorticoids in regions of murine brain

Girard T (GirT) corticosteroid hydrazones (corticosterone (CORT) and 11-dehydrocorticosterone (11DHC)) were most abundant in the cortex, hippocampus and amygdala with significant lower CORT/11DHC ratios observed upon transgenic disruption of the enzyme primarily caused by a significant accumulation of 11DHC. (**a**) Histological image of cryosection of murine brain stained with haematoxylin and eosin with the outline of the MSI-LESA regions of interest (ROIs) (cortex; hippocampus, HPC; and amygdala, Am). (**b, d**) Heat map distribution by MALDI-FTICR-MSI of GirT-CORT derivative at *m/z* 460.31698±0.025Da in wild type (**b**) and 11β-HSD1$^{-/-}$ (**d**) mice. (**c,e**) Heat map distribution by MALDI-FTICR-MSI of GirT-11DHC derivative at *m/z* 458.30133±0.025Da in wild type (**c**) and 11β-HSD1$^{-/-}$ (**e**) mice. Signal intensity is depicted by color on the scale shown. Scale bar (2mm). **cps** = count per second. (**f**) CORT/11DHC ratios measured by MALDI-FTICR-MSI (MSI), LC-MS/MS and LESA in regions of interest in murine brain were

significantly lower in 11β-HSD1$^{-/-}$mice (KO) than wild-type (WT) ($p<0.001$ overall between genotypes). (**g**) Differences between genotypes in CORT/11DHC ratios were caused by a statistically significant increase of 11DHC and a trend to a similar magnitude of reduction in CORT in 11β-HSD1$^{-/-}$ mice, measured in whole brain by LC-MS/MS. Statistical analysis was by two-way ANOVA for LESA and MSI and Student's t-test for LC-MS/MS and absolute measurements (n=12). Data are mean ± SEM. *P<0.05, ** P<0.01 and *** P<0.001.

Europe PMC Funders Author Manuscripts

Europe PMC Funders Author Manuscripts

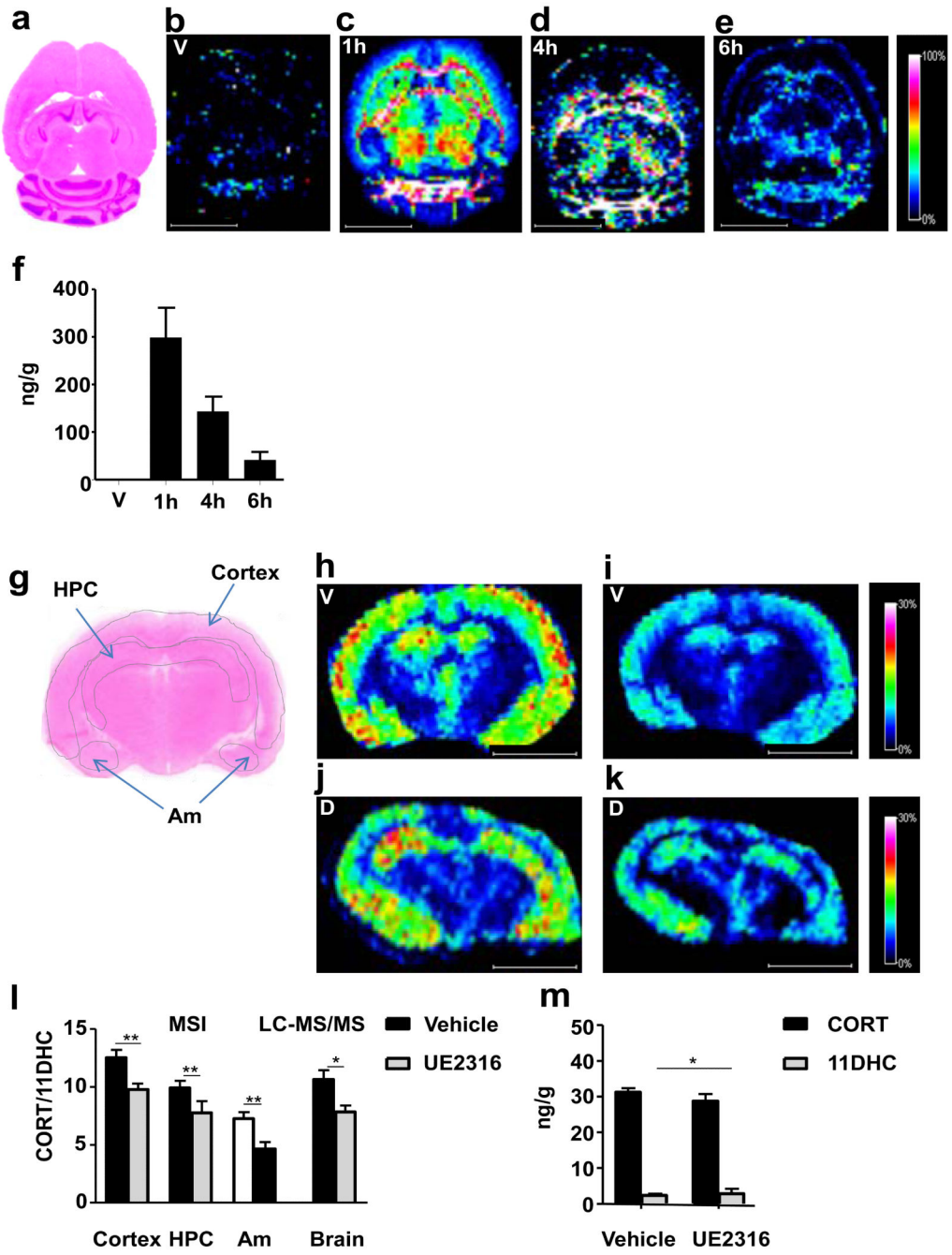

Figure 3. Effect of pharmacological inhibition of 11β-hydroxysteroid dehydrogenase type 1 (11β-HSD1) with UE2316 in C57BL/6 mice

Girard T (GirT) derivatives (corticosterone (CORT) and 11-dehydrocorticosterone (11DHC)) were mostly distributed across the cortex, hippocampus and amygdala, after enzyme inhibition, CORT/11DHC ratios showed a significant decline as a result of an increased 11DHC metabolite. (**a**) Histological image of horizontal cryosection of murine brain stained with haematoxylin and eosin. (**b-e**) MSI heat map distribution of *m/z* 390.08377±0.025Da representing UE2316 in brain over a 6h time course in mice receiving Vehicle (V) or UE2316 (D). (**f**) Amounts of UE2316 in whole brain measured by LC-

MS/MS demonstrated the same temporal pattern as those determined by MSI. (**g**) Histological image of coronal cryosection of murine brain stained with haematoxylin and eosin with the outline of the MSI regions of interest (ROIs) (cortex; hippocampus, HPC; and amygdala, Am). (**h, j**) MSI heat map of GirT-CORT at *m/z* 460.31698±0.005Da brain from mice receiving Vehicle (**h**) or UE2316 (1h post dose) (**j**). (**i, k**) GirT-11DHC at *m/z* 458.30133±0.025Da in brain from mice receiving Vehicle (**i**) or UE2316 (**k**). Signal intensity is depicted by color on the scale shown. Scale bar (2mm). **cps** = count per second. (**h**) A significant decline ($p<0.01$, overall between groups) in CORT/11DHC ratios was observed across the ROIs by MSI in the brain after administration of UE2316, showing good agreement with data generated by LC-MS/MS in whole brain. (**i**) Absolute quantification of corticosteroids in brain tissue by LC-MS/MS showed that the differences in CORT/11DHC ratios were associated with a statistically significant increase of 11DHC and a trend to a decrease in CORT in UE2316-treated mice. Statistical analysis was performed using two-way ANOVA for MSI and Student's t-test for LC-MS/MS and absolute measurements (n=12). Data are mean ± SEM. *P<0.05, ** and P<0.01.

Europe PMC Funders Author Manuscripts

Europe PMC Funders Author Manuscripts

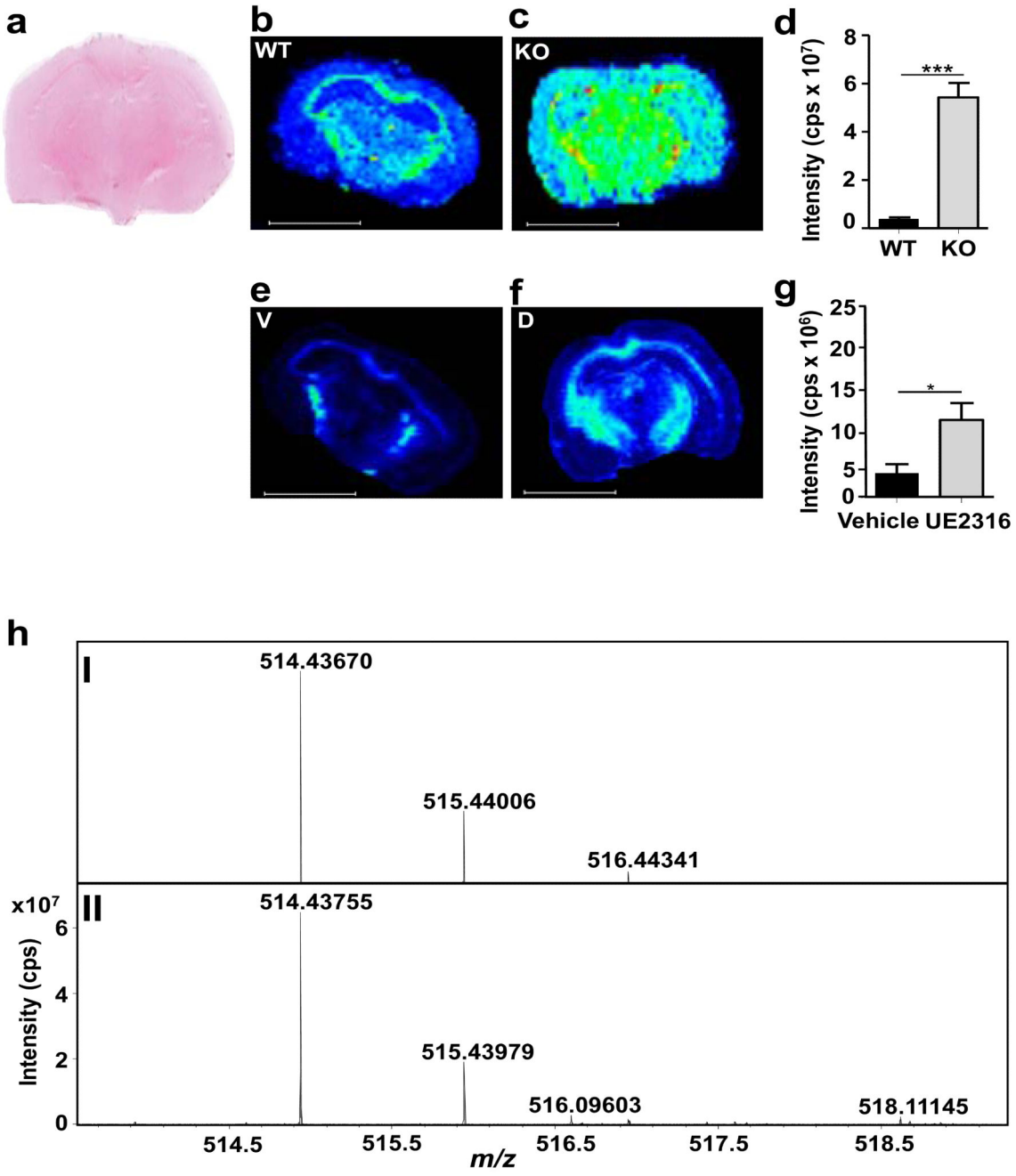

Figure 4. MSI detection of 7-ketocholesterol, an alternative substrate for 11β-HSD1

A significant increase in Girard T 7-ketocholesterol (GirT-7KC) intensity was observed across the whole brain in mice after transgenic disruption of 11β-HSD1$^{-/-}$ (KO) and after administration of UE2316 (1 h post-dose). (**a**) Histological image of coronal cryosection of murine brain stained with haematoxylin and eosin. MSI heat map of GirT-KC at *m/z* 514.43670±0.025Da in (**b**) wild type (WT), (**c**) 11β-HSD1$^{-/-}$ and brain from mice receiving (**e**) Vehicle (V) or (**f**) UE2316. Quantification of MSI signal intensity for GirT-7KC across the whole brain for (**d**) wild type versus 11β-HSD1$^{-/-}$ mice and for (**g**) mice treated with

vehicle of UE2316. (**h**). (**I**) Theoretical monoisotopic distribution of GirT-7KC; and (**II**) GirT-KC in mouse brain. GirT-7KC was detected in murine brain and its levels increased in 11β-HSD1$^{-/-}$ mice (**c**) and following inhibition of the enzyme using UE2316 (**f**). Signal intensity is depicted by color on the scale shown. Scale bar (2mm). **cps** = counts per second. Statistical analysis was performed using two way ANOVA (n=12). Data are mean ± SEM. *P<0.05 and *** P<0.001.

Europe PMC Funders Author Manuscripts